Smart Structures and Systems, *Vol. 29, No. 3 (2022) 475-484*
https://doi.org/10.12989/sss.2022.29.3.475

A cable tension identification technology using percussion sound

Guowei Wang [1,2a], Wensheng Lu [1,2b], Cheng Yuan [1,2c] and Qingzhao Kong*[1,2]

[1] *State Key Laboratory of Disaster Reduction in Civil Engineering, Tongji University, Shanghai, China*
[2] *Department of Disaster Mitigation for Structures, Tongji University, Shanghai, China*

(*Received April 22, 2021, Revised December 9, 2021, Accepted October 20, 2021*)

Abstract. The loss of cable tension for civil infrastructure reduces structural bearing capacity and causes harmful deformation of structures. Currently, most of the structural health monitoring (SHM) approaches for cables rely on contact transducers. This paper proposes a cable tension identification technology using percussion sound, which provides a fast determination of steel cable tension without physical contact between cables and sensors. Notably, inspired by the concept of tensioning strings for piano tuning, this proposed technology predicts cable tension value by deep learning assisted classification of "percussion" sound from tapping a steel cable. To simulate the non-linear mapping of human ears to sound and to better quantify the minor changes in the high-frequency bands of the sound spectrum generated by percussions, Mel-frequency cepstral coefficients (MFCCs) were extracted as acoustic features to train the deep learning network. A convolutional neural network (CNN) with four convolutional layers and two global pooling layers was employed to identify the cable tension in a certain designed range. Moreover, theoretical and finite element methods (FEM) were conducted to prove the feasibility of the proposed technology. Finally, the identification performance of the proposed technology was experimentally investigated. Overall, results show that the proposed percussion-based technology has great potentials for estimating cable tension for *in-situ* structural safety assessment.

Keywords: cable tension identification; deep learning; percussion sound; structural health monitoring

1. Introduction

Steel cables have been widely used in civil infrastructures due to its light-to-weight ratio and high strength capacity. Typical applications include stay cables in long-span bridges, vertical and horizontal cables in point-supported cable-net curtain walls, slings in suspension bridges, and cable-net roofs in various stadiums. During long-term service of cable structures, the change of cable tension may bring harmful deformation and reduce the bearing capacity of the structure. Cable condition assessment has become an essential aspect in structural maintenance process.

Traditional cable tension estimation methods can be divided into direct measurement and indirect measurement (Kim *et al*. 2020). The direct method obtains cable tension by using measuring devices installed at the end of the cable or enclose the cable surface, such as load cells, hydraulic jacks, and Elasto-Magnetic (EM) sensors (Cappello *et al*. 2018, Sumitro *et al*. 2005). The indirect method mainly uses a vibration-based approach, which can relatively get a fast cable tension estimation compared to direct methods (Caetano 2011, Geier *et al*. 2006, Kim *et al*. 2017, Li *et al*. 2014, Shinke *et al*. 1980, Zui *et al*. 1996). The vibration-based method computes the natural frequency of the cable under excitation and estimates the tension by establishing the relationship between frequency and cable tension. Notably, several acceleration sensors need to be used to measure the dynamic response, which causes the following limitations: (i) Installation of extensive sensors is time-consuming and cost-ineffective; (ii) Performance of deployed sensors may be influenced by the *in-situ* environmental conditions.

To overcome the current problems in the steel cable tension estimation, a few recently developed methods have been proposed. On the one hand, novel sensing devices and sensing technologies have been applied in real-scale structures, such as Elasto-Magneto-Electric (EME) Sensors (Zhang *et al*. 2018b), Portable PZT-Interface Technique (Huynh and Kim 2014), Fiber Bragg Grating (FBG) sensors (Hu *et al*. 2017), FBG force-testing ring (Li *et al*. 2015), the smart FRP-OF-FBG cable (He *et al*. 2013). While these new techniques represent valuable tools to evaluate cable tension, the relatively complicated sensor installation in advance still limits its applications. On the other hand, the non-contact measurement methods have attracted increasing attention in recent decades. These methods capture the displacement time history curves during cable vibration and compute the cable forces from the resonance frequencies. For instance, the use of cameras to determine cable tension (Du *et al*. 2020, Kim *et al*. 2017, Xu *et al*. 2018, Yang *et al*. 2019), the use of microwave interferometric radar to estimate the cable tension in a long-span cable-stayed bridge (Bartoli *et al*. 2008, Zhang *et al*. 2020a, Zhao *et al*.

*Corresponding author, Professor,
E-mail: qkong@tongji.edu.cn
[a] Ph.D. Student, E-mail: guowei@tongji.edu.cn
[b] Professor, E-mail: wally@tongji.edu.cn
[c] Ph.D., E-mail: 20310146@tongji.edu.cn

ISSN: 1738-1584 (Print), 1738-1991 (Online)

2020), and the application of Laser Doppler technology (Nassif *et al*. 2005) have been reported. The detection accuracy of current vision-based measurements is often affected by the intensity of light and weather. Besides, most of the reported vision-based approaches require artificial markers on each cable before measurements, which highly reduces the test efficiency. Though the reported cable tension estimation accuracy of long-span bridges by using the above-mentioned methods could exceed 95% (Bao *et al*. 2017, Feng *et al*. 2017, Wang *et al*. 2015), the tested cables have to be excited with sufficient vibration prior to measurements.

Inspired by the concept of tensioning strings for piano tuning, this paper proposes a novel technology using percussion sounds to identify the tension of steel cables. Steel cable serving in different tension values generates unique tones of sound when it is tapped by impact hammers. To better understand the mechanism among impact, vibration, and sounding, analytical studies and numerical simulations were firstly performed to reveal the relationship between cable tension and natural frequency. Subsequently, a series of "percussion" tests were investigated under different cable tension values. Mel-frequency cepstral coefficients (MFCCs) extracted from sounds as acoustic features to train the proposed CNN network for tension identification. Therefore, the cable force estimation method based on acoustic features (MFCCs) and deep learning (CNN) is a potential method, especially for infrastructures with small-span cables and complex boundary conditions. Nevertheless, as far as the author knows, there is no report in the relevant literature at present.

2. Methodologies

Acoustic-based approaches have shown great potentials in structural health monitoring, which include bolt loosening monitoring (Kong *et al*. 2018), cup-lock scaffolds looseness detection, fault diagnosis for rolling bearings (Wang *et al*. 2020c), early warning of hazard for pipelines (Wan and Mita 2010), and metal fatigue crack detection (Li *et al*. 2020, Wang *et al*. 2020b). Most of the aforementioned approaches apply Acoustic Emission (AE) sensors and do not directly analyze the sound signals generated by the acoustic waves. Significantly, it is quite difficult to establish the relationship between tensions and percussion sounds by using theoretical or mathematical methods. And the deep learning approaches offer the possibility to construct percussion sounds to cable tensions prediction model. Specifically, the 2D CNN framework was selected in this study since its ability to adaptively extract features from high-dimensional data, improve parameters sharing and connection sparsity, and dramatically enhance the effectiveness of feature classification. As a consequence, the technology of cable tension identification is proposed based on the processing of sound signals, which mainly includes two steps. As shown in Fig. 1, the first step is to establish a database of percussion sounds from tapping steel cables under different tension conditions. After that, an optimized CNN framework is employed for classifying percussion sounds and determining cable tension levels. During the CNN training, MFCCs features of percussion sounds are extracted and divided into training and testing datasets. To achieve the precise prediction, deep network parameters are optimized based on the training accuracy and final prediction results are stored in the cable tension database.

2.1 MFCCs features extraction

Since the obtained percussion sounds contain noise components, it is crucial to extract proper features from sound data to ensure the accuracy of the prediction. MFCCs have been proven as an effective tool to extract acoustic features for structural damage identification (Cheng *et al*.

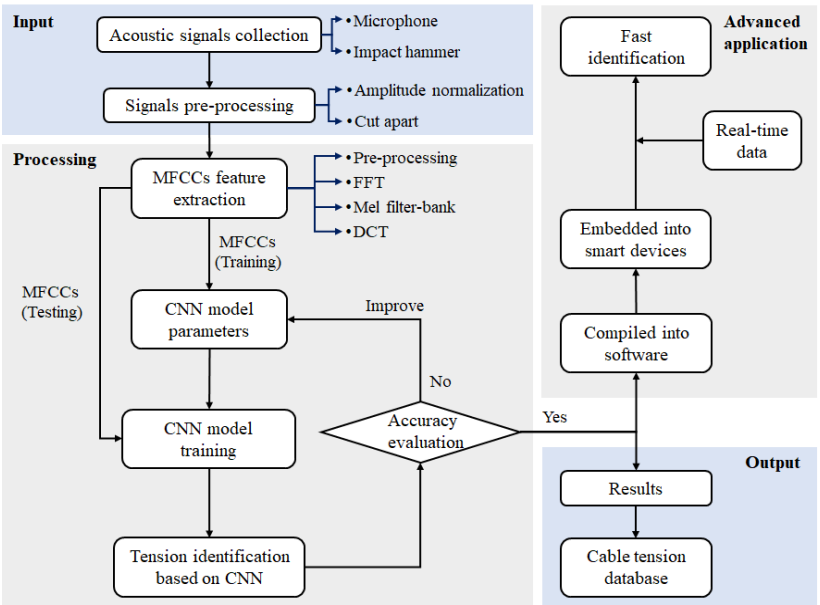

Fig. 1 The flowchart of the proposed cable tension identification technology

2020, Dai 2016, Wang *et al*. 2020a, Yuan *et al*. 2021). It has to be remarked that the MFCCs features can simulate the non-linear mapping of human ears to sound and retain intact important information about sound signals generated by the cable under percussion. Specifically, MFCCs allow better mitigate insignificant changes in the high bands of the energy spectrum. An example of a sound signal, its MFCCs extraction process is described in Fig. 2. After pre-emphasis, framing, and windows of the input audio signal in the time domain to avoid energy leakage, the fast Fourier transform (FFT) is employed to obtain the signal's energy distribution in the frequency spectrum (Zhang *et al*. 2018a). Subsequently, we apply the frequency spectrum passes a Mel-filter bank composed of a series of triangular filters. Finally, by taking the magnitudes' logarithm at each of the Mel-frequencies and utilizing the Discrete Cosine Transform (DCT), we obtain the MFCCs features. The more specific extraction steps are as follows:

(1) Pre-processing: The pre-processing process can be divided into three steps: pre-emphasis, framing, and windows. Compared with the initial input signal, Pre-emphasis increases the magnitude of higher frequencies. To maintain the sound frequency contours, the signal is split into short-time frames and the Hamming windows function is applied to each frame. We can realize these steps through

$$\hat{s}(n) = \hat{s}(n) \times \alpha s(n-1) \qquad 0.95 < \alpha < 0.99 \tag{1}$$

$$\begin{cases} s'(n) = \hat{s}(n) \times w(n) \\ w(n) = 0.54 - 0.46cos(2\pi n/L - 1) \\ 0 \le n \le L-1 \end{cases} \tag{2}$$

where $\hat{s}(n)$ is a sequence of frames after framing operation, α is the pre-emphasis ratio, whose value is usually taken as 0.98, and L denotes the Hamming window length. Following the FFT performed on the pre-processed signal $\hat{s}(n)$, the spectrum can be calculated using Eqs. (3)-(4), where $X(k)$ is a complex number for each of N frequency bands representing magnitude, and $P(k)$ represents the power spectrum of each frame.

$$X(k) = \sum_{n=1}^{N} s'(n) exp\left(-j\frac{2\pi kn}{N}\right) \qquad 1 \le k \le N \tag{3}$$

$$P(k) = \frac{1}{N}|X(k)|^2 \tag{4}$$

(2) Mel-filter bank filtering: As shown in Fig. 2, these filters are non-uniformly spaced on the frequency axis, that is to say, fewer filters in high-frequency regions. The mapping relationship between Mel-frequency f_{mel} and frequency f_{Hz} in the filter bank can be described by Eq. (5).

$$f_{mel} = 1127ln\left(1 + \frac{f_{Hz}}{700}\right) \tag{5}$$

A Mel-filter bank filters the frequency spectrum computed from the previous step to obtain the Mel-spectrum $X'(k)$. This process can be achieved by the following equations

$$X'(k) = \sum_{k=1}^{N} H(k)|X(k)|^2 \tag{6}$$

$$H(k) = \begin{cases} 0 & k < f(m-1) \\ \dfrac{k - f(m-1)}{f(m)} & f(m-1) \le k \le f(m) \\ \dfrac{f(m+1) - k}{f(m+1) - f(m)} & f(m) \le k \le f(m+1) \\ 0 & k > f(m+1) \end{cases} \tag{7}$$

where $0 \le m \le M$, M is the number of filters, and the center frequency is $f(m)$, and $H(k)$ denotes a set of created triangular filters.

Typically, Mel-spectrum peaks denote dominant frequency components of the sound signal connected by a smooth curve (see Fig. 2), which refers to the spectral envelope. Consequently, a spectrum consists of a spectral envelope $E(k) = |X(k)|^2$ and spectral details $H(k)$, which can be expressed in the following form

$$|X'(k)| = H(k) \times E(k) \tag{8}$$

(3) Logarithm operation: Calculate the log magnitude of each Mel-filter bank output $|X'(k)|$ according to Eq. (9). This step intends to make features less variable to acoustic coupling variations

$$ln|X'(k)| = ln|H(k)| + ln|E(k)| \tag{9}$$

(4) Discrete cosine transform (DCT): we can separate spectral envelope and spectral details by DCT. Taking $ln|X'(k)|$ into Eq.(10) yields the time domain signal $X'(k)$, which is significantly different from the original signal. Finally, apply a low-frequency filter to $X'(k)$ can obtain $e(k)$, and the vectors of $e(k)$ forms MFCCs are features of sound signals. The DCT process can be expressed as shown in Eqs. (10) and (11)

$$x'(k) = \sum_{m=0}^{M-1} ln[X'(k)]cos\left[n(k-0.5)\frac{\pi}{M}\right] \qquad n = 0,1,\ldots j \tag{10}$$

$$x'(k) = h(k) + e(k) \tag{11}$$

2.2 Convolutional Neural Network (CNN)

CNN, as a deep learning network, was first proposed by LeCun *et al*. (1998) and applied to document recognition. With the rapid progress of computing hardware and data processing approach, the CNN offers a few approaches to data classification and regression from the massive dataset

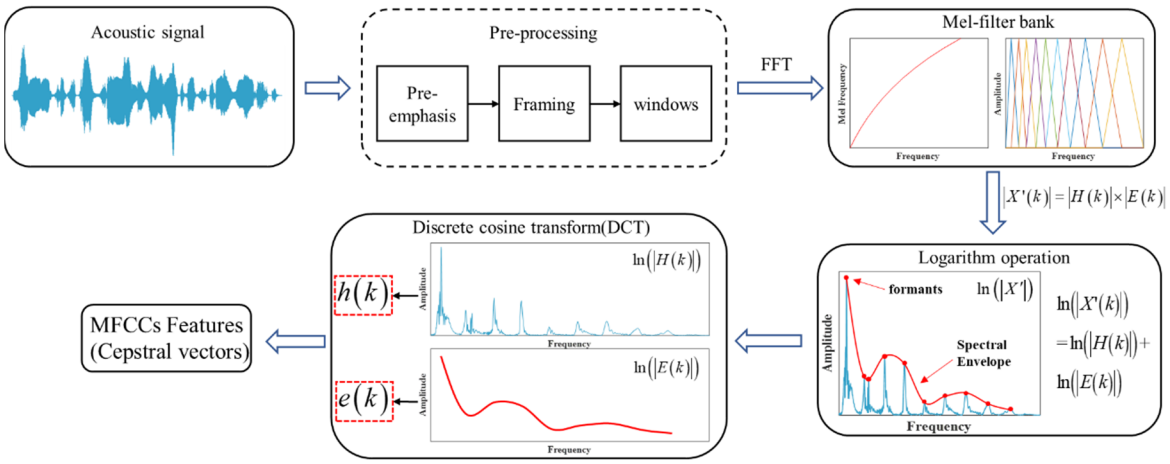

Fig. 2 MFCCs features extraction flowchart

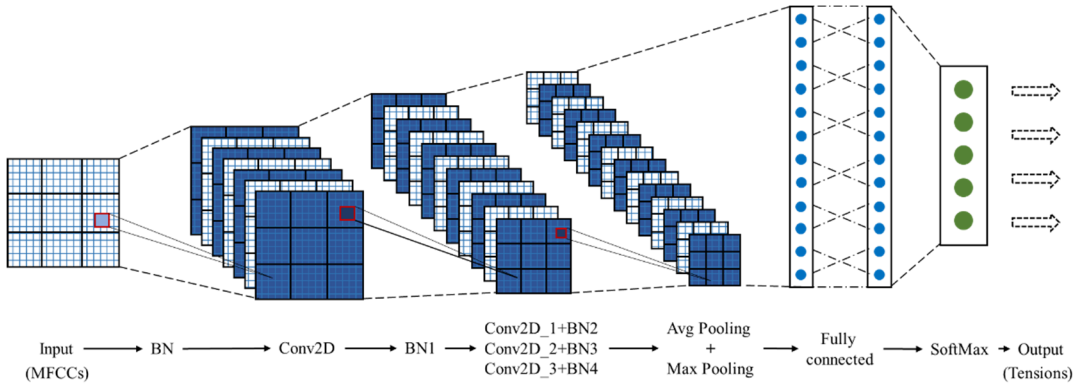

Fig. 3 The architecture of the proposed CNN model

(Lecun *et al*. 1998, Tang *et al*. 2019, Tome *et al*. 2019, Ye *et al*. 2019). For example, Modarres *et al*. (2018) developed a CNN-based approach to identify the existence and type of structural damage. Xin *et al*. (2020) applied CNN to construct the relationship between scalograms of acoustic emission signal and bridge status. Santos *et al*. (2016) presented an online damage detection technique based on a deep learning algorithm for structure. It is worth noting that CNN combines computational speed and accuracy when analyzing databases obtained from the percussion sounds, and ensures that cable tensions can be identified efficiently in applications. Compared with traditional artificial neural network (ANN), CNN contains a feature extractor composed of convolutional layers and pooling layers (Dai 2016). A set of convolution kernels, as well as several feature maps, form the convolutional layer. The principal purpose of setting convolutional layers is to extract input data features, and various sizes of kernels can obtain different feature information. Moreover, the pooling layers are used to reduce feature maps' dimensions but preserve the significant information. These procedures simplify the complexity of networks and enhance the generalization ability of the model.

The CNN architecture for cable tension identification proposed in this research is given in Fig. 3. The framework composes of an input layer, four convolutional layers, two pooling layers, a fully connected layer, and an output layer. As we have mentioned before, the convolutional layer performs the calculation on input data, and Eq. (12) shows this process (Yarotsky 2017)

$$h_{l+1} = ReLU(W_l h_l + b_l) \tag{12}$$

where h_l, W_l, and b_l is the value of representing the output, weight matrix, and bias of the l th layer, respectively, and ReLU is the active function.

In addition, the dropout algorithm is utilized after each convolution calculation to debase the risk of over-fitting. Subsequently, the feature maps after batch normalization are decreased in dimension through average pooling and maximum pooling. Furthermore, the reduced feature maps are converted into training output through the fully connected layer and the SoftMax function. Finally, Calculated the loos function $J(W,b)$ according to the training output and update the parameters W and b of the networks through the gradient descent algorithm. The optimization operation is as follows

$$\begin{aligned} W_l &= W_l - \lambda \frac{\partial J(W,b)}{\partial W_l} \\ b_l &= b_l - \lambda \frac{\partial J(W,b)}{\partial b_l} \end{aligned} \tag{13}$$

where λ is the learning rate. Notably, CNN is continuously

(a) For cable length of 290 mm

(b) For cable length of 575 mm

Fig. 4 The numerical models and first-order frequencies of cables with two lengths under 1 kN tension

trained until the loss function converges to the optimal value.

2.3 Relationship between cable tension and percussion-induced vibration

To the best of our knowledge, percussion signal properties due to cable vibration are highly determined by cable natural frequencies. In terms of the slim-short cables, such as cable-supported facades or roofs (Patterson 2011, Zhang *et al*. 2020b). Flat taut string theory is utilized to demonstrate the relationship between cable tension and natural frequencies (Kim and Park 2007). The cable tension T can be computed as follows

$$T = 4mL_c^2\left(\frac{f_n}{n}\right)^2 \tag{14}$$

where m, L_c, m and f_n denote the mass per unit length, length, order of calculation, and natural frequency of cable, respectively. The first-order natural frequencies of two lengths' cables are computed by Eq. (14), and listed in Table 1. Specifically, a numerical model is established adopting the tension-only element "Link 10" in software ANSYS. The cable with fixed boundary conditions at both ends and subjected to axial tension is divided into 12 parts. To realize the pretension of the cable, an initial strain is applied to the element. As an example, the frequencies of cables with lengths of 290 mm and 575 mm under the tension of 1 kN are shown in Figs. 4(a)-(b) respectively.

As seen in Table 1, the natural frequencies increase with the increase of cable tension. Meanwhile, under the same cable tension degree, the frequencies decrease with the increase of the cable length. Consulting the working mechanism of the piano, piano tones are generated by vibrating strings. The measured vibration frequency values f_n are used for piano tuning. In this research, f_n refers to the vibrational frequency of a cable. Analytical and numerical studies conducted a preliminary study to prove that it could be a possible solution to recognize the cable tension using percussion sound.

Table 1 Frequencies calculated by string theory and FEM under different tensions

Test No.	Cable tension (kN)	Length (mm)			
		290		575	
		Theory (Hz)	FEM (Hz)	Theory (Hz)	FEM (Hz)
1	1	81.25	80.22	41.02	40.58
2	10	256.99	253.62	129.61	127.91
3	20	363.62	358.67	183.39	180.89
4	30	445.57	439.28	224.72	221.55
5	40	514.76	507.24	259.62	255.82
6	50	575.81	567.11	290.41	286.02

3. Experimental study

3.1 Experimental setups

To validate the proposed cable tension identification technology, experimental verifications were carried out. As shown in Fig. 5, the experimental setup mainly includes a loading servo-hydraulic tester, a set of acquisition equipment (the power amplifier, I/O device, and compact DAQ), an impact hammer, and a microphone.

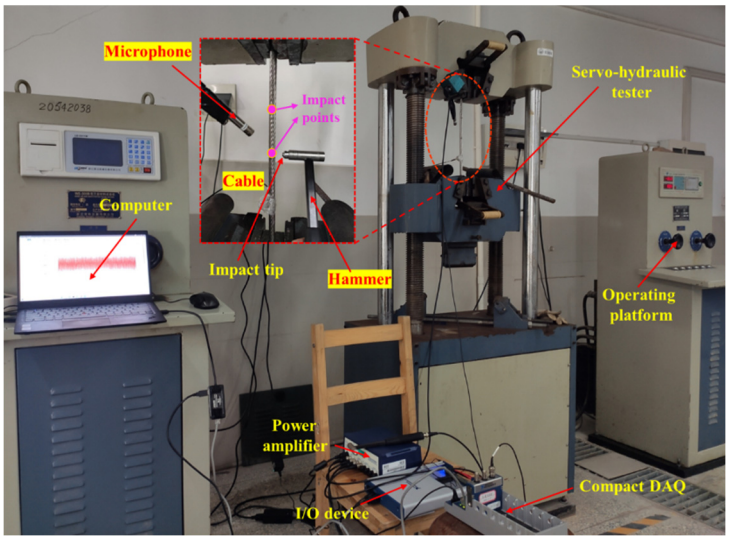

Fig. 5 Experimental setup

As shown in Eq. (14), the cable tension T is directly related to parameters m, L_c, and f_n. Therefore, the cable samples with two lengths (sample 1: 290 mm × 10 mm, sample 2: 575 mm × 10 mm), labeled as 290 and 575, were prepared for percussion tests. Meanwhile, to simulate the fixed boundary condition when cable serves, test cables were applied with a pre-tightening tension with chuck. A microphone with a sampling rate of 20 kHz was set to collect percussion sounds generated by hammer tapping. To investigate the influences of hammer head material on identification accuracy, two impact heads with different materials (metal and nylon) were investigated for all tests.

3.2 Test procedures

The percussion sound dataset, as depicted in Table 2, was divided into six categories (i.e., 1 kN, 10 kN, 20 kN, 30 kN, 40 kN, 50 kN). The percussion signals were manually labeled by a combination of tension, length, and material. The experiment was done by randomly tapping one-half or one-quarter of the cable 50-70 times under each tension degree via the hammer mounted with a metal or nylon impact tip. Notably, this experiment differs from the traditional test procedure in that tapping times are artificially altered with the aim of introducing certain randomness in the dataset to enhance the adaptability of the prediction model. We split the sound signals into 100-140 segments for simplification with 0.7s, and the process was shown in Fig. 6. Totally, 2652 sound signals were prepared for the dataset.

3.3 Cable tension identification using CNN

As mentioned previously, to effectively extract depth information from the dataset and conduct precise prediction, a CNN model was proposed, and the detailed parameters were listed in Table 3. Notably, by comparison with a basic CNN model, the proposed CNN architecture substituted the pooling layer after each convolutional layer with the global pooling layers after all convolution operations were completed to simplify the number of parameters. Besides, we randomly selected 80% and 20% of the experiment data as the training dataset and validation dataset individually to

Table 2 The dataset of sound categories

Sound categories dataset No.	Sound categories abbreviations	Labels	Numbers	Total numbers
1	1-290-Me	1 kN	102	2652
	1-290-Ny	1 kN	137	
	1-575-Me	1 kN	101	
	1-575-Ny	1 kN	102	
2	10-290-Me	10 kN	101	
	10-290-Ny	10 kN	109	
	10-575-Me	10 kN	113	
	10-575-Ny	10 kN	130	
3	20-290-Me	20 kN	101	
	20-290-Ny	20 kN	111	
	20-575-Me	20 kN	124	
	20-575-Ny	20 kN	112	
4	30-290-Me	30 kN	102	
	30-290-Ny	30 kN	102	
	30-575-Me	30 kN	120	
	30-575-Ny	30 kN	123	
5	40-290-Me	40 kN	100	
	40-290-Ny	40 kN	101	
	40-575-Me	40 kN	113	
	40-575-Ny	40 kN	118	
6	50-290-Me	50 kN	104	
	50-290-Ny	50 kN	102	
	50-575-Me	50 kN	108	
	50-575-Ny	50 kN	116	

Table 3 CNN model node parameters

Layer (Type)	Output Shape	Parameters
input (Input)	(None, 40, 259, 1), Batch size = 16	0
batch normalization (BN)	(None, 40, 259, 1)	4
conv2d (Conv2D)	(None, 40, 259, 10)	90
batch normalization_1 (BN1)	(None, 40, 259, 10)	40
dropout (Dropout)	(None, 40, 259, 10)	0
conv2d_1 (Conv2D)	(None, 20, 130, 20)	1800
batch normalization_2 (BN2)	(None, 20, 130, 20)	80
dropout_1 (Dropout1)	(None, 20, 130, 20)	0
conv2d_2 (Conv2D)	(None, 10, 65, 50)	9000
batch_normalization_3 (BN3)	(None, 10, 65, 50)	200
dropout_2 (Dropout2)	(None, 10, 65, 50)	0
conv2d_3 (Conv2D)	(None, 5, 33, 100)	45000
batch_normalization_4 (BN4)	(None, 5, 33, 100)	400
dropout_3 (Dropout3)	(None, 5, 33, 100)	0
global_average_pooling2d (Avg Pooling)	(None, 100)	0
global_max_pooling2d (Max Pooling)	(None, 100)	0
concatenate (Concatenate)	(None, 200)	0
dense (Dense)	(None, 1000)	200000
dropout_4 (Dropout4)	(None, 1000)	0
dense_1 (Dense1)	(None, 6)	6006

repeatedly train the model.

Following the MFCCs features extraction procedure, the original one-dimensional signal was transformed into a spectrum representing acoustic features in the time-frequency domain. In the CNN training and testing phase, we fed the MFCCs features corresponding to per signal data into the CNN model as summarized in Fig. 6. Firstly, the size of the input feature maps was 1@40 × 259 (channels@width × height). After four convolutional layers and two global pooling layers, the feature map size was dropped to 100@5 × 33. Then, these decreased-dimensional feature maps were transmitted to the fully connected layer. Finally, the probability expression of the prediction results, namely the cable tension, was determined by the SoftMax function.

4. Results and discussion

Fig. 7 illustrates the training/testing process (overall loss and accuracy) and cable tension identification results of the proposed CNN model after 100 iterations. All sound signals and sound with only metal tips were used as two training datasets, whose corresponding tests (denoted as T1 and T2) were the sound only with nylon tips and six sets of untrained sound (i.e., 20 segments from each cable tension degree), respectively. The CNN model was trained and validated with 80% and 20% of the dataset individually. The learning rate is 0.003, and the minibatch size is set to 10 (Yu and Chen 1997). Simultaneously, the loss function in training is the Cross-Entropy (CE) criterion, which is employed to compute the error between the estimated cable tension and the real results. Overall, the curves fluctuate up and down, related to the number of the overall dataset. As shown in Fig. 7(a), with the increasing of iterations, the accuracy of training and testing was approximately 1.0, respectively. Conversely, the loss value decreases to 0.0. To investigate the influences of hammer head material, the trained CNN using only sound signals with the metal tip was tested by sound signals with the nylon tip, and the cable

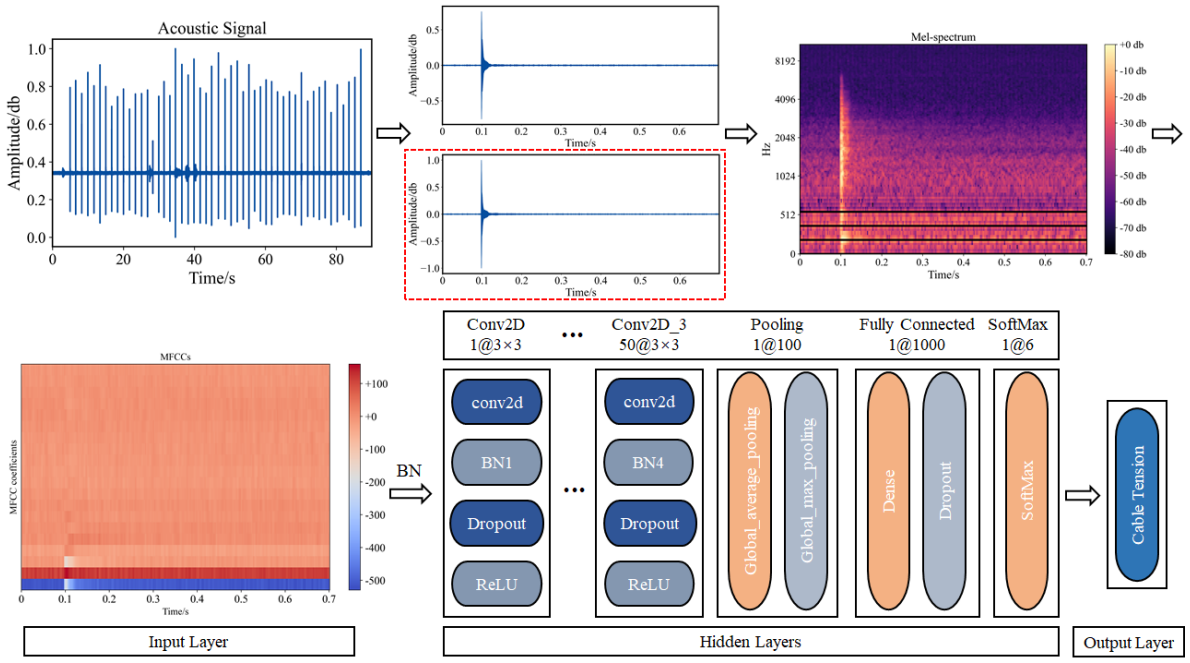

Fig. 6 Cable tension identification

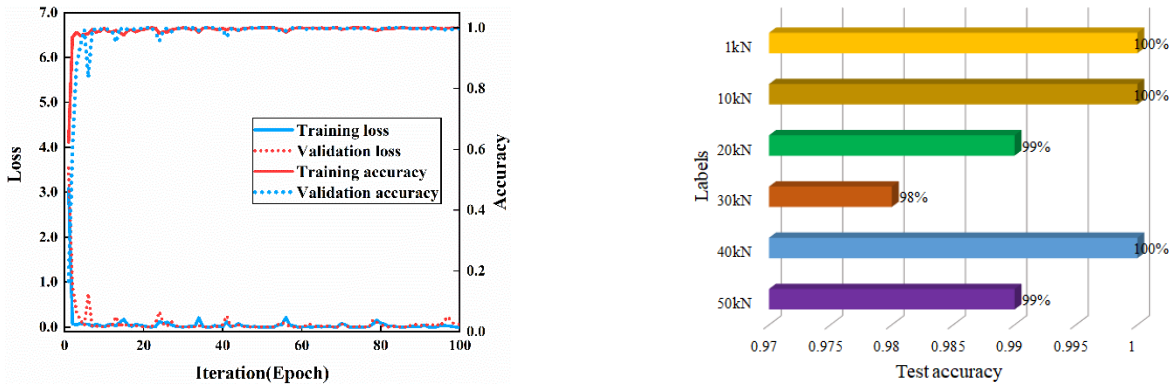

(a) Training dataset: all sound signals; testing dataset: six untrained dataset signals

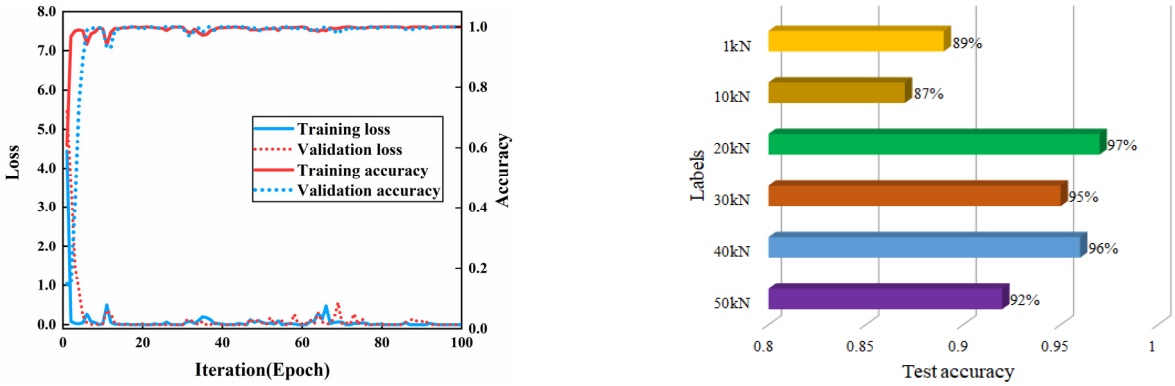

(b) Training dataset: sound signals with the metal tip; testing dataset: sound signals with the nylon tip

Fig. 7 Training/testing process and cable tension identification results of the proposed CNN

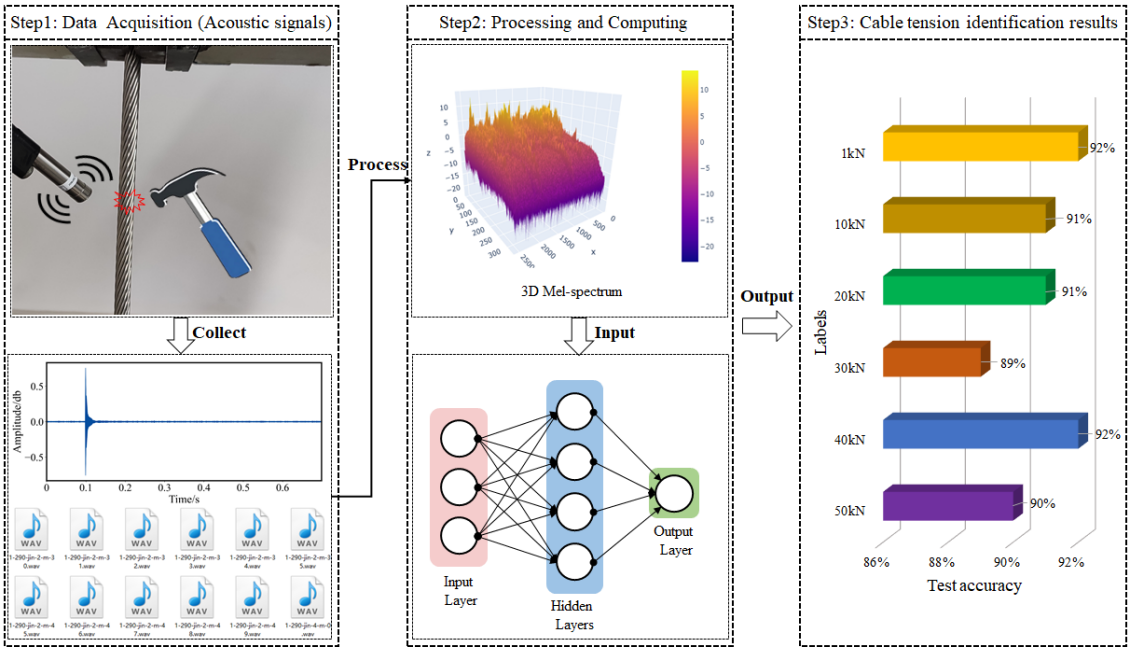

Fig. 8 Results of the proposed CNN and an overview of the novel method

tension identification results are depicted in Fig. 7(b). Overall, the testing average accuracy for T1 is 99.33%, and the high accuracy is also achieved on T2 with 92.67%, which indicates that the effect of hammer head material on identification accuracy is almost negligible.

On the one hand, the accuracy rate can reflect the performance of a CNN model. The higher the accuracy rate, the better the performance of the model. On the other hand, in some cases, such as uneven sample distribution, the accuracy rate cannot truly reflect CNN's performance.

Consequently, we artificially add noise to part of sound signals in the dataset as new input data to visible the robustness of CNN. It is evident that the proposed CNN model has high accuracy in the six categories of cable tension identification even in the presence of various noise, as shown in Fig. 8. For instance, the highest and lowest identification accuracy rates from 1 kN to 40 kN reach 92% and 89%, respectively. The prediction results demonstrate that MFCCs can well describe the features of a sound signal generated by cable vibration, and CNN can effectively capture the dynamic changes of the acoustic features of signals. In addition, the processing step could be further compiled into software and embedded in portable devices for fast data processing and cable tension condition assessment.

5. Conclusions

In this paper, a steel cable tension identification method using acoustic features and deep learning is proposed. When a steel cable is excited by impact, it generates different sounds with the change of its tension. Analytical and numerical studies show the relationship between the cable natural frequencies and cable tension. To further validate the proposed method, a series of tests were carried out to collect sound data from different cable tension conditions. A developed CNN model was tested with the only sound with a nylon tip and six untrained dataset signals, respectively. Results show that the average accuracy of the cable tension identification in two tests (T1 and T2) reaches 96%. In future work, sound data will be greatly enriched with the consideration of different cable diameters, and the hammer and microphone will be improved and installed on cable-climbing robots or drones to achieve automatic cable tension estimation. Moreover, it ought to be further optimized to improve the current model with shorter time-consuming and high precision.

Acknowledgments

This research is financially supported by National Key Research Program of China (Grant No. 2020YFC1512500), National Natural Science Foundation of China (Grant Nos. 51638012 and 51978507), Science and Technology Commission of Shanghai Municipality (Grant No. 19DZ1201200), and Innovation Foundation for Universities Collaboration of Shandong Province (Grant No. XTZ201903).

Declaration of conflicting interests

The authors declared no potential conflicts of interest with respect to the research, authorship, and publication of this article.

References

Bao, Y., Shi, Z., Beck, J.L., Li, H. and Hou, T.Y. (2017), "Identification of time-varying cable tension forces based on adaptive sparse time-frequency analysis of cable vibrations", *Struct. Control Health Monitor.*, **24**(3), e1889. https://doi.org/10.1002/stc.1889

Bartoli, G., Facchini, L., Pieraccini, M., Fratini, M. and Atzeni, C. (2008), "Experimental utilization of interferometric radar techniques for structural monitoring", *Struct. Control Health Monitor.*, **15**(3), 283-298. https://doi.org/10.1002/stc.252

Caetano, E. (2011), *On the Identification of Cable Force from Vibration Measurements*, IABSE-IASS Symposium, London, UK.

Cappello, C., Zonta, D., Laasri, H.A., Glisic, B. and Wang, M. (2018), "Calibration of elasto-magnetic sensors on in-service cable-stayed bridges for stress monitoring", *Sensors* (*Basel*), **18**(2), p. 466. https://doi.org/10.3390/s18020466

Cheng, H., Wang, F., Huo, L. and Song, G. (2020), "Detection of sand deposition in pipeline using percussion, voice recognition, and support vector machine", *Struct. Health Monitor.*, **19**(6), 2075-2090. https://doi.org/10.1177/1475921720918890

Dai, W. (2016), "Acoustic scene recognition with deep learning", *Detection and classification of acoustic scenes and events* (*DCASE*) *challenge*, Carnegie Mellon University, Pittsburg, PA, USA.

Du, W., Lei, D., Bai, P., Zhu, F. and Huang, Z. (2020), "Dynamic measurement of stay-cable force using digital image techniques", *Measurement*, **151**. https://doi.org/10.1016/j.measurement.2019.107211

Feng, D., Scarangello, T., Feng, M.Q. and Ye, Q. (2017), "Cable tension force estimate using novel noncontact vision-based sensor", *Measurement*, **99**, 44-52. https://doi.org/10.1016/j.measurement.2016.12.020

Geier, R., De Roeck, G. and Flesch, R. (2006), "Accurate cable force determination using ambient vibration measurements", *Struct. Infrastr. Eng.*, **2**(1), 43-52. https://doi.org/10.1080/15732470500253123

He, J., Zhou, Z. and Jinping, O. (2013), "Optic fiber sensor-based smart bridge cable with functionality of self-sensing", *Mech. Syst. Signal Process.*, **35**(1-2), 84-94. https://doi.org/10.1016/j.ymssp.2012.08.022

Hu, D., Guo, Y., Chen, X. and Zhang, C. (2017), "Cable force health monitoring of Tongwamen bridge based on fiber Bragg grating", *Appl. Sci.*, **7**(4), p. 384. https://doi.org/10.3390/app7040384

Huynh, T.-C. and Kim, J.-T. (2014), "Impedance-based cable force monitoring in tendon-anchorage using portable PZT-interface technique", *Mathe. Problems Eng.*, **2014**, 1-11. https://doi.org/10.1155/2014/784731

Kim, B.H. and Park, T. (2007), "Estimation of cable tension force using the frequency-based system identification method", *J. Sound Vib.*, **304**(3-5), 660-676. https://doi.org/10.1016/j.jsv.2007.03.012

Kim, S.-W., Jeon, B.-G., Cheung, J.-H., Kim, S.-D. and Park, J.-B. (2017), "Stay cable tension estimation using a vision-based monitoring system under various weather conditions", *J. Civil Struct. Health Monitor.*, **7**(3), 343-357. https://doi.org/10.1007/s13349-017-0226-7

Kim, S.W., Cheung, J.H., Park, J.B. and Na, S.O. (2020), "Image-based back analysis for tension estimation of suspension bridge hanger cables", *Struct. Control Health Monitor.*, **27**(4), e2508. https://doi.org/10.1002/stc.2508

Kong, Q., Zhu, J., Ho, S.C.M. and Song, G. (2018), "Tapping and listening: a new approach to bolt looseness monitoring", *Smart Mater. Struct.*, **27**(7), p. 07LT02. https://doi.org/10.1088/1361-665X/aac962

Lecun, Y., Bottou, L., Bengio, Y. and Haffner, P. (1998), "Gradient-based learning applied to document recognition", *Proceedings of the IEEE*, **86**(11), 2278-2324.

https://doi.org/10.1109/5.726791
Li, H., Zhang, F. and Jin, Y. (2014), "Real-time identification of time-varying tension in stay cables by monitoring cable transversal acceleration", *Struct. Control Health Monitor.*, **21**(7), 1100-1117. https://doi.org/10.1002/stc.1634
Li, X.-X., Ren, W.-X. and Bi, K.-M. (2015), "FBG force-testing ring for bridge cable force monitoring and temperature compensation", *Sensors Actuators A: Phys.*, **223**, 105-113. https://doi.org/10.1016/j.sna.2015.01.003
Li, N., Wang, F. and Song, G. (2020), "New entropy-based vibro-acoustic modulation method for metal fatigue crack detection: An exploratory study", *Measurement*, **150**, p. 107075. https://doi.org/10.1016/j.measurement.2019.107075
Modarres, C., Astorga, N., Droguett, E.L. and Meruane, V. (2018), "Convolutional neural networks for automated damage recognition and damage type identification", *Struct. Control Health Monitor.*, **25**(10), p. e2230. https://doi.org/10.1002/stc.2230
Nassif, H.H., Gindy, M. and Davis, J. (2005), "Comparison of laser Doppler vibrometer with contact sensors for monitoring bridge deflection and vibration", *NDT & E Int.*, **38**(3), 213-218. https://doi.org/10.1016/j.ndteint.2004.06.012
Patterson, M. (2011), *Structural Glass Facades and Enclosures*, John Wiley & Sons.
Santos, J.P., Cremona, C., Calado, L., Silveira, P. and Orcesi, A.D. (2016), "On-line unsupervised detection of early damage", *Struct. Control Health Monitor.*, **23**(7), 1047-1069. https://doi.org/10.1002/stc.1825
Shinke, T., Hironaka, K., Zui, H. and Nishimura, H. (1980), "Practical formulas for estimation of cable tension by vibration method", *Proceedings of the Japan Society of Civil Engineers*, **1980**(294), 25-32. https://doi.org/10.2208/jscej1969.1980.294_25
Sumitro, S., Kurokawa, S., Shimano, K. and Wang, M.L. (2005), "Monitoring based maintenance utilizing actual stress sensory technology", *Smart Mater. Struct.*, **14**(3), S68-S78. https://doi.org/10.1088/0964-1726/14/3/009
Tang, Z., Chen, Z., Bao, Y. and Li, H. (2019), "Convolutional neural network-based data anomaly detection method using multiple information for structural health monitoring", *Struct. Control Health Monitor.*, **26**(1), p. e2296. https://doi.org/10.1002/stc.2296
Tome, E.S., Pimentel, M. and Figueiras, J. (2019), "Online early damage detection and localisation using multivariate data analysis: Application to a cable-stayed bridge", *Struct. Control Health Monitor.*, **26**(11), p. e2434. https://doi.org/10.1002/stc.2434
Wan, C. and Mita, A. (2010), "Early warning of hazard for pipelines by acoustic recognition using principal component analysis and one-class support vector machines", *Smart Struct. Syst., Int. J.*, **6**(4), 405-421. https://doi.org/10.12989/sss.2010.6.4.405
Wang, L., Zhang, X., Huang, S. and Li, L. (2015), "Measured frequency for the estimation of cable force by vibration method", *J. Eng. Mech.*, **141**(2), p. 06014020. https://doi.org/10.1061/(asce)em.1943-7889.0000890
Wang, F., Song, G. and Mo, Y.L. (2020a), "Shear loading detection of through bolts in bridge structures using a percussion-based one-dimensional memory-augmented convolutional neural network", *Comput.-Aid. Civil Infrastr. Eng.*, **36**(3), 289-301. https://doi.org/10.1111/mice.12602
Wang, K., Cao, W., Su, Z., Wang, P., Zhang, X., Chen, L., Guan, R. and Lu, Y. (2020b), "Structural health monitoring of high-speed railway tracks using diffuse ultrasonic wave-based condition contrast: theory and validation", *Smart Struct. Syst., Int. J.*, **26**(2), 227-239. https://doi.org/10.12989/sss.2020.26.2.227
Wang, R., Liu, F., Hou, F., Jiang, W., Hou, Q. and Yu, L. (2020c), "A non-contact fault diagnosis method for rolling bearings based on acoustic imaging and convolutional neural networks", *IEEE Access*, **8**, 132761-132774. https://doi.org/10.1109/access.2020.3010272
Xin, H., Cheng, L., Diender, R. and Veljkovic, M. (2020), "Fracture acoustic emission signals identification of stay cables in bridge engineering application using deep transfer learning and wavelet analysis", *Advances in Bridge Engineering*, ***1***(1). https://doi.org/10.1186/s43251-020-00006-7
Xu, Y., Brownjohn, J. and Kong, D. (2018), "A non-contact vision-based system for multipoint displacement monitoring in a cable-stayed footbridge", *Struct. Control Health Monitor.*, **25**(5), p. e2155. https://doi.org/10.1002/stc.2155
Yang, Y., Sanchez, L., Zhang, H., Roeder, A., Bowlan, J., Crochet, J., Farrar, C. and Mascarenas, D. (2019), "Estimation of full-field, full-order experimental modal model of cable vibration from digital video measurements with physics-guided unsupervised machine learning and computer vision", *Struct. Control Health Monitor.*, **26**(6), p. e2358. https://doi.org/10.1002/stc.2358
Yarotsky, D. (2017), "Error bounds for approximations with deep ReLU networks", *Neural Netw*, **94**, 103-114. https://doi.org/10.1016/j.neunet.2017.07.002
Ye, X., Jin, T. and Yun, C. (2019), "A review on deep learning-based structural health monitoring of civil infrastructures", *Smart Struct. Syst., Int. J.*, **24**(5), 567-585. https://doi.org/10.12989/sss.2019.24.5.567
Yu, X.-H. and Chen, G.-A. (1997), "Efficient backpropagation learning using optimal learning rate and momentum", *Neural Networks*, **10**(3), 517-527. https://doi.org/10.1016/s0893-6080(96)00102-5
Yuan, C., Zhang, J., Chen, L., Xu, J. and Kong, Q. (2021), "Timber moisture detection using wavelet packet decomposition and convolutional neural network", *Smart Mater. Struct.*, **30**(3), p. 035022. https://doi.org/10.1088/1361-665X/abdc08
Zhang, Q., Lin, J., Song, H. and Sheng, G. (2018a), *Fault Identification based on PD Ultrasonic Signal using RNN, DNN and CNN*, 2018 Condition Monitoring and Diagnosis (CMD), https://doi.org/10.1109/CMD.2018.8535878
Zhang, R., Duan, Y., Zhao, Y. and He, X. (2018b), "Temperature compensation of elasto-magneto-electric (EME) sensors in cable force monitoring using BP neural network", *Sensors (Basel)*, **18**(7), p. 2176. https://doi.org/10.3390/s18072176
Zhang, G., Wu, Y., Zhao, W. and Zhang, J. (2020a), "Radar-based multipoint displacement measurements of a 1200-m-long suspension bridge", *ISPRS J. Photogram. Remote Sensing*, **167**, 71-84. https://doi.org/10.1016/j.isprsjprs.2020.06.017
Zhang, P., Zhu, H., Lu, W., Lu, X. and MacRae, G.A. (2020b), "Vibration analysis of shallow cable with horizontal spring and dashpot at one end", *Eng. Struct.*, **211**, p. 110452. https://doi.org/10.1016/j.engstruct.2020.110452
Zhao, W., Zhang, G. and Zhang, J. (2020), "Cable force estimation of a long-span cable-stayed bridge with microwave interferometric radar", *Comput.-Aid. Civil Infrastr. Eng.*, **35**(12), 1419-1433. https://doi.org/10.1111/mice.12557
Zui, H., Shinke, T. and Namita, Y. (1996), "Practical formulas for estimation of cable tension by vibration method", *J. Struct. Eng.*, **122**(6), 651-656. https://doi.org/10.1061/(asce)0733-9445(1996)122:6(651)

BS